Article

A Study on Decisive Early Stages in White Etching Crack Formation Induced by Lubrication

Jürgen Wranik [1,2,*], **Walter Holweger** [2,3], **Tarek Lutz** [4], **Philipp Albrecht** [4], **Benedikt Reichel** [4] and **Ling Wang** [2]

1   Zeller+Gmelin GmbH & Co. KG, Schlossstraße 20, 73054 Eislingen/Fils, Germany
2   National Centre for Advanced Tribology at Southampton (nCATS), Mechanical Engineering Department, School of Engineering, Faculty of Engineering and Physical Sciences, University of Southampton, Southampton SO17 1BJ, UK; walter.holweger@t-online.de (W.H.); ling.wang@soton.ac.uk (L.W.)
3   Technology Consultant, Sailegärten 2, 72351 Erlaheim, Germany
4   NMI Natural and Medical Sciences Institute at the University of Tübingen, Markwiesenstr. 55, 72770 Reutlingen, Germany; tarek.lutz@nmi.de (T.L.); philipp.albrecht@nmi.de (P.A.); benedikt.reichel@nmi.de (B.R.)
*   Correspondence: j.wranik@zeller-gmelin.de

Abstract: The reliability of rolling bearings is affected by white etching crack (WEC) or white structure flaking (WSF) failures, causing tremendous commercial burdens for bearing manufacturers and operators. The research for the underlying failure mechanism has attracted interest from a large scientific community over decades. Despite the significant amount of efforts, a root cause of white etching cracking is still missing. Amongst other factors, lubricant chemistry is considered to be essential in WEC formation. The authors aim to elucidate this key parameter by provoking white etching crack formation on a FE8 bearing test rig using a well-described set of chemicals in high- and low-reference lubricants. Scanning electron microscopy and energy dispersive X-ray analysis prove the presence of a patchy tribofilm on the surface of bearing washers, leading most likely to a higher frictional torque at the early stages of operation when the low reference oil is used. Secondary neutral mass spectrometry (SNMS) shows a hydrogen containing tribofilm in the shallow subsurface of about 30 nm depth, suggesting that hydrogen proliferating into bearing material may subsequently facilitate crack propagation via dislocation pileups, leading to premature bearing failure.

Keywords: tribology; bearing failure; white etching cracks

1. Introduction

Bearings are key elements in drive trains in industrial and automotive applications, whose life is found to be significantly shortened by a widely known failure mode called White Etching Cracking (WEC). WEC phenomena were firstly reported in 1966 as subsurface cracks with microstructural changes adjacent to them and observed by sectioning of a bearing [1]. The area with microstructural changes appears to be white under the light of an optical microscope after the surface observed is etched with nitric acid in ethanol (Nital). WEC has been reported to appear in bearings in many industrial and automotive applications [2–6], but especially in the steadily growing wind energy industry [7]. Due to its unpredictable nature, WEC caused failures that have been suggested to be one of the most critical causes leading to a large downtime of wind turbines, and resulting in repair costs of EUR >250,000 per failure [8]. The impact of WEC failures has led to global research efforts to understand the failure mechanisms and develop solutions preventing them from occurring. Among the research community residual electrical current, boundary lubrication, lubricant chemistry and hydrogen are discussed as possible main drivers for this phenomenon [9,10]. Studies on the influence of lubricant chemistry are often based on readily formulated lubricants or confidential compositions, which makes it difficult to draw clear conclusions concerning the impact of lubricant chemistry on WEC creation.

From the chemical analyses and information on components reported within these studies, zinc dithiophosphate, as an antiwear component, and calcium sulfonate, as a corrosion inhibitor, have been identified as promotors in WEC formation by several studies [11–19]. To understand the role of lubricant chemistry on WEC creation, this study uses chemically well-described formulations such as zinc- di(2-ethylhexyl)dithiophosphate (ZDDP) in polyalphaolefine (PAO). As dicyclohexylamine (DCHA) is widely used in bearing technology as part of multifunctional additives or corrosion protection, this substance is also included in this work. PAO itself is reported not to lead to WEC [15] and is therefore employed as a high-reference lubricant within this work. Laboratory tests have been conducted on an FE8, a widely used test rig for studying WEC creation [13,15,17,20]. By switching experiments from low-reference to high-reference lubricants and vice versa, other researchers have shown a big impact of early stages in the WEC evolution process [12]. Earlier research from the authors shows changes in the subsurface material structure, such as the occurrence of pores in low-reference bearing samples in the early stages in front of the first appearance of subsurface WEC features as well [21]. This study aims to investigate these decisive early stages of WEC evolution in order to gain new insights on the WEC formation process. Within this research approach, frictional torque sensor data are compared for both low- and high-reference test runs, aiming especially at how they differ in the early stages of the test runs. Bearing samples from intentionally stopped tests are analysed by Secondary Neutral Mass Spectrometry (SNMS), Scanning Electron Microscopy (SEM) and Energy Dispersive X-ray spectrometry (EDX) to determine possible differences in the surface allocation of a tribofilm formation. To obtain information on hydrogen in the tested bearing, samples of them were immersed in liquid nitrogen immediately after being dismounted from the test rig and analysed by SNMS.

2. Materials and Methods

2.1. FE8 Cylindrical Roller Bearing Test Rig

A standard FE8 test rig (Schaeffler Technologies AG & Co. KG, Schweinfurt, Germany) (DIN 51 819-3) is used for the tests. The rig tests the ability of lubricants to withstand boundary lubrication [22] (Figure 1). In order to maintain a constant bearing temperature, a fan for the test head and a heat exchanger for the lubricant oil are used. The temperature of the two bearings passed by the lubricant is recorded by contacting the stationary housing washer with thermocouples. The torque on the FE8 test rig is measured by an in-line torque transducer, which records the required force to hold the test head housing (Figure 1). The torque is the product of this force and the distance from the point of action (0.12 m) [23]. As a result, this records all frictional torque, including those from the two auxiliary bearings that are essential to absorb mechanical forces in a radial direction (13 in Figure 2) and is proportional to the frictional torque of the test bearings [24].

To set the axial load, the test head is placed into a mounting press and the desired axial load is controlled by a load cell. A schematic of the test head is shown in Figure 2.

Two cylindrical roller thrust bearings (CRTB) (Schaeffler Technologies AG & Co. KG, Schweinfurt, Germany) defined as 81212 (according to DIN 722, Material AISI 52100) standards are used for each test. Each bearing contains a stationary housing washer, a rotating shaft washer and a brass cage holding 15 rolling elements in place. A round-robin test under WEC conditions conducted by [20] shows an equal propensity of each bearing to fail due to WEC. Nevertheless, there is an indication that the shaft washer of bearing seems to form surface anomalies earlier than that of the housing washer. Prior to testing, the bearings are cleaned carefully by flushing with heptane, then with isopropanol and again with heptane (0.1 L each solvent, quality analytical grade) to ensure the absence of residues from machining lubricants or corrosion inhibitors on the surface. The surface roughness of both the rolling element and the bearing washer is analysed according to the ISO 4287/2009 standard using a Zeiss/Accretech Surfcom Touch 50 device (Carl-Zeiss QEC GmbH, Ostfildern, Germany). The evaluation length was 5 mm, with a measuring range of 500 μm and a measuring velocity of 0.15 mm/s. Root mean square surface roughness (Rq)

was 0.05 μm for the washer and 0.07 μm for the rolling element. The FE8 test rig conditions are set to 60 kN loading on the test bearings, 750 revolutions per minute (rpm) and 100 °C bearings temperature, similar to the tests reported in [13,15,17] where WEC has been studied. These settings and the utilisation of lubricants with a given viscosity–temperature behaviour (Table 1) results in an expanded and adjusted rating life, according to ISO 281, of 120 h and a minimum film thickness, according to Dowson and Higginson [25], of 0.046 μm. The λ-value as a relationship of the minimum film thickness and the root mean square surface roughness of the rolling element and washer produced results of 0.53; hence the tests were conducted under boundary lubrication.
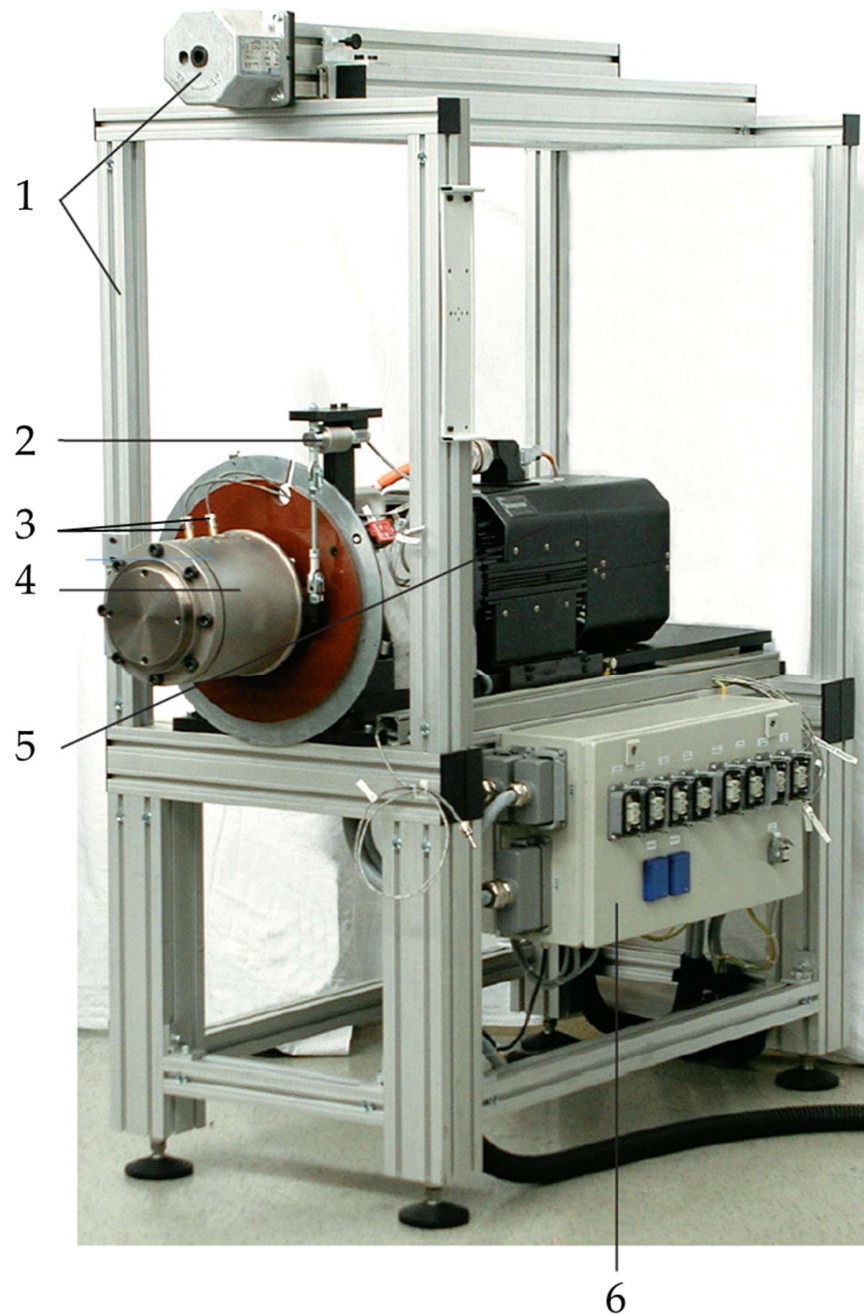

Figure 1. Structure of the FE8 test rig: 1. Frame and crane for the test head. 2. Torque transducer 3. Thermocouples for each bearing. 4. Test head. 5. Driving unit 6. Control cabinet for terminals for cooling, fan heating. Figure adapted with permission from Ref. [23] Copyright 2017, Schaeffler Technologies AG & Co.
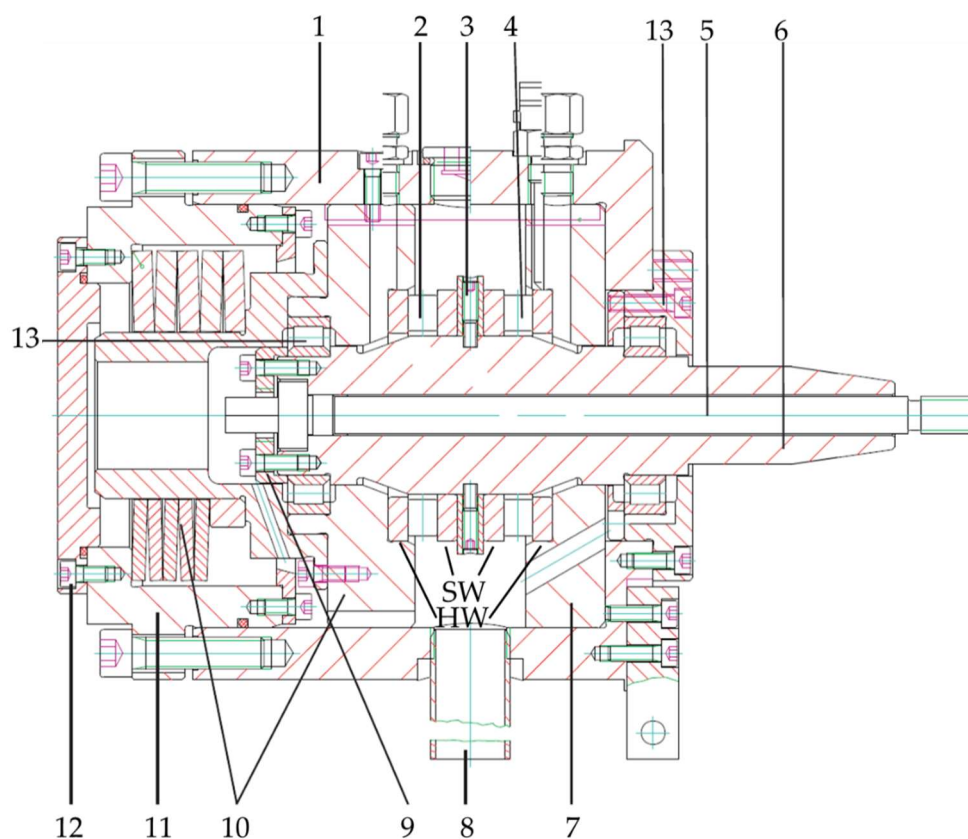
Figure 2. Test head with axial cylindrical roller bearings. 1. Housing. 2. Test bearing 2 (test head sided bearing). 3. Spacer 4. Test bearing 1 (motor sided bearing). 5. Shaft. 6. Clamping bolt. 7. Bearing seat. 8. Drain pipe. 9. Cap. 10. Bearing support with screwed-on pilot pin. 11. Lid cup of spring package. 12. Lid. 13. Auxiliary bearing. Both test bearings consist of a stationary housing (HW) and a rotating shaft washer (SW). Figure adapted with permission from Ref. [23] Copyright 2017, Schaeffler Technologies AG & Co.

Table 1. Analysed values of the PAO used in this study.

Parameter	Standard	Durasyn 168
Optical assessment		no colour, clear, no sludge
Colour	DIN ISO 2049	L0.5
Viscosity 40 °C [mm^2/s]	ASTM D 7042	46.3
Viscosity 100 °C [mm^2/s]	ASTM D 7042	7.85
Viscosity index [-]	ASTM D 2270	140
Density 15 °C [g/cm^3]	DIN EN ISO 12185	0.832
Refractive index [-]	DIN 51423-2	1.4621
Water content (procedure C) [ppm]	DIN 51777	46
TAN [mg KOH/g]	DIN EN 12634	<0.1
Insoluble in petrol (10 μm) [%]		0.01
Insoluble in petrol (5 μm) [%]		0.06
Insoluble in petrol (1.2 μm) [%]		0.06
Insoluble in petrol (0.8 μm) [%]		0.07
Conductivity [pS/m]	DIN 51412-1	0.02

2.2. Lubricants and Their Chemistry

2.2.1. Polyalphaolefine (PAO)

The PAO used for this study is registered in the EU under EC 500-183-1. The data being measured are given in Table 1. Traces of metallic components in the magnitude of 1–3 ppm are found using inductive coupled plasma atomic emission spectrometry. The

PAO is used as the high reference oil as well as the base stock for the low reference oils in this study.

2.2.2. Zinc Dithiophosphate (ZDDP)

The ZDDP used is an undiluted zinc di(2-ethylhexyl)dithiophosphate (EC list no. 224-235-5). It is used as one of the additives for the low reference oils.

2.2.3. Dicyclohexylamine (DCHA)

The DCHA used is guaranteed to be >99% pure with a water content below 0.3% and registered according to EC 202-980-7. It is the second additive for the low reference oils in this study.

2.2.4. The Lubricants

Three oils, including one high-reference (HR) and two low-reference (LR1 and LR2) oils have been tested in this study. Table 2 provides compositions of the three oils and details of the preparation are given below:

1. The high-reference lubricant (HR) consists solely of PAO, as described in Section 2.2.1.
2. The two low-reference oils (LR1 and LR2) are produced by mixing the components (adding ZDDP then DCHA for LR2 into PAO) and stirring at 40 °C for 10 min in a quantity of 7 kg. The 2.5% of ZDDP used here is typical for a gear oil formulation [26]. The water content of LR1 and LR2 prior to the test run was below 100 ppm (DIN 51777, Karl Fischer indirect titration).

Table 2. Preparation used as lubricants in the test runs.

Lubricant Tag	(PAO) [%]	w (ZDDP) [%]	w (DCHA) [%] w
HR	100		
LR1	97.5	2.5	
LR2	95	2.5	2.5

2.3. SNMS

SNMS is utilized to measure the elemental composition in the tribofilm on the tested bearing surface, including hydrogen. Depth profiles of the chemical composition was obtained through sputtering. With its relatively large focal spot, it analyses a comparatively large area with a high ionisation yield. This avoids the problems coming up by the use of high lateral resolving techniques, e.g., Secondary Ion Mass Spectrometry (SIMS). The device INA 3 from Leybold/Specs was used, with an aperture diameter of 7.5 mm, a distance of 2.5 mm and a sputtering rate of 0.52 nm/s. The bearings were immediately dismounted after the tests, cleaned by flushing with heptane, isopropanol and again with heptane before they were immersed in liquid nitrogen to limit the escaping of hydrogen from the sample. The timespan between the termination of the tests and suspending the bearings in liquid nitrogen was about 20 min. To gain sample sizes measurable in SNMS (approx. 2×2 cm^2), the bearing washers were crushed with the help of a hydraulic press directly out of the nitrogen container in radial direction. This measure avoided additional sources for impurities and warming by a cutting technique. For safety reasons, it is necessary to shield the bearing with a metal cover while crushing (Figure 3).
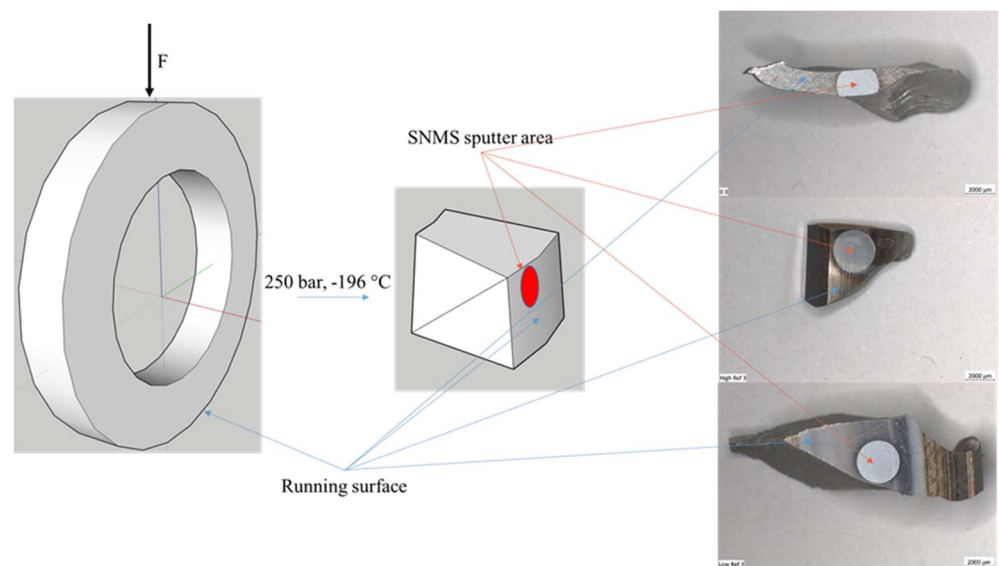
Figure 3. Specimen prepared by means of cryogenic crushing with the aid of a hydraulic press (principle arrangement (**left**)) and resulting pieces (**right**).

2.4. Scanning Electron Microscopy (SEM) and Energy Dispersive X-ray Spectrometry (EDX)

In order to visualise the different areas of the bearing surface, SEM pictures were taken with a Zeiss Auriga device and an in-lens-detector (Carl Zeiss Microscopy Deutschland GmbH, Oberkochen, Germany). To get information on the composition of these spots, EDX measurements with a voltage of 5 kV and an image width of 75 μm are taken. Whereas SNMS results in depth profiles, EDX mapping of eligible elements are conducted on the individual measuring positions in order to reveal the lateral distribution.

3. Results

3.1. FE8 Test Runs

The tests were either conducted until:

1. The complete failure of the bearing indicated by exceeding a torque threshold;
2. A first pitting, detected by an acceleration sensor mounted on the test head;
3. A manual termination at distinct time steps.

The threshold for the vibration measured by an accelerometer mounted on the test head was defined based on the multiplication of a steady state noise by a factor of 16, whereas the steady-state noise was recorded after 24 h. The factor of 16 was chosen to ensure pitting occurs based on experience of previous tests. Table 3 gives an overview of the conducted test runs.

Table 3. Overview of FE8 test runs.

Test Run Tag	Running Time [hh:mm]	Termination Method	WEC y/n
LR1-1	159:11	Torque > 35 Nm	y
LR2-1	72:15	Torque > 35 Nm	y
LR2-2	32:30	Acceleration sensor >16	y
LR2-3	25:00	Manually	y
LR2-4	20:00	Manually	n
LR2-5	03:00	Manually	n
HR1	160:42	Torque > 35 Nm	n
HR2	137:47	Torque > 35 Nm	n
HR3	03:00	Manually	n.d.

Karl-Fischer titration in order to determine water content of fresh and used lubricants (DIN 51777, indirect titration) leads in each case to values below 100 ppm (w/w).

Torque Responses

Figure 4 shows the responses of the torque sensor for the tests not being terminated in a very early stage. The torque level for the HR tests is much lower than that of the LR ones, whereas the non-WEC tests show much lower torque in the bearings than that of the WEC ones. The differences start to occur at about 20 min from the start of the tests, and there is an approximate 20% torque increase in the LR 1 and LR2 tests compared with that of the two HR tests. However, the high torque values of the tests with low reference lubricants decrease over the course of the tests and converge slowly to the level of the HR tests.
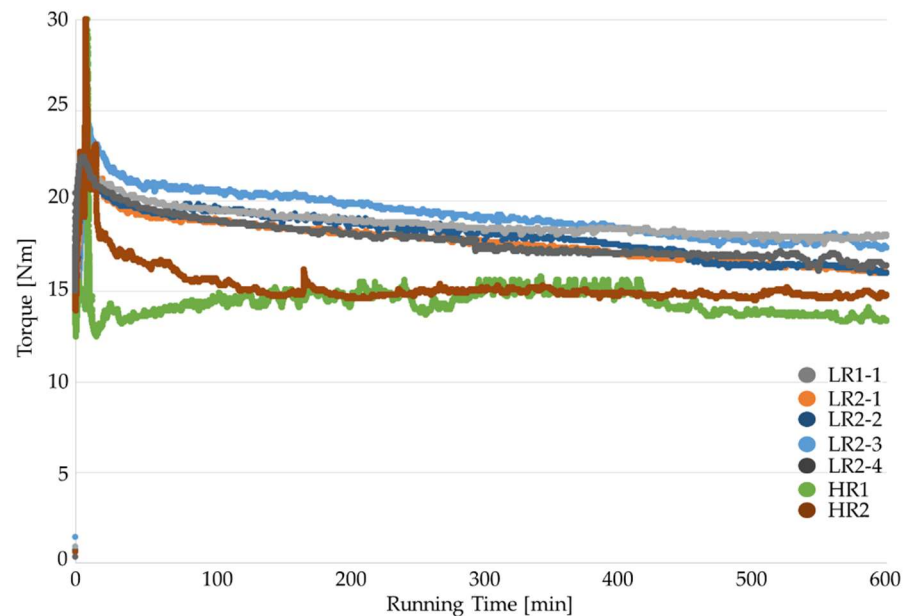

Figure 4. Torque responses during the FE8 tests between 0 and 600 min.

Figure 5 shows the torque responses for the LR2-5 and HR3 during the 180 min of testing, highlighting the significant difference in bearing torqued between the tests lubricated by the high- and low-reference oils.
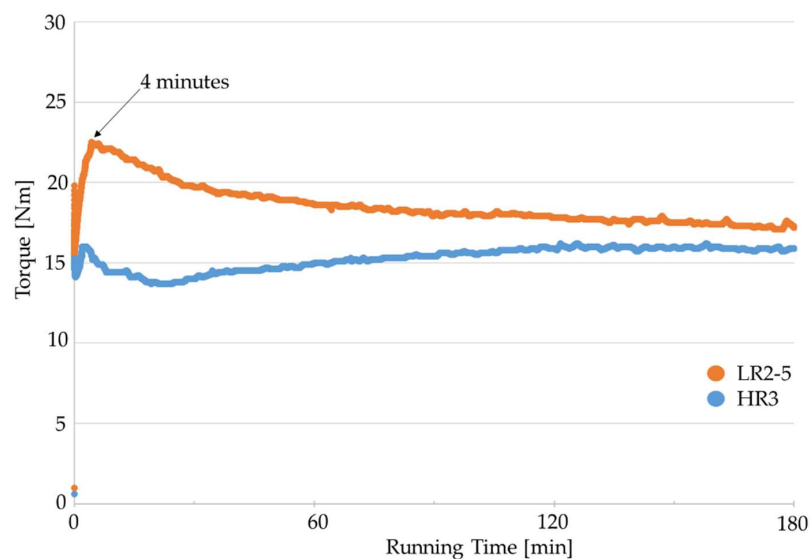

Figure 5. Torque values of early interrupted tests. Maximum difference between the test run LR2-6 (PAO/ZDDP/DCHA) and HR3 (PAO) at 4 min with an increased torque value by 57%.

A statistical evaluation of the torque responses shows a mean torque of 15.0 Nm in the case of the HR-test runs (HR1, 2, 3), between 20 and 180 min testing and with a coefficient of variation of 6.0%. The mean torque of the LR2 test runs in the same time span, resulting in 19.5 Nm, with a coefficient of variation of 4.6%. Interpreting the significance of these differences a disadvantage of the test head design that has to be considered as the load is applied at room temperature. Elevated temperatures (Table 4) in the case of LR2 compared to HR1 test runs may lead to a higher material extension and thus to an increased load and higher friction torque. Nevertheless, a comparison of the raw data at the maximum bearing temperature of the HR-test runs with those of LR-test runs (Table 4) shows significantly higher torque values for the LR test runs, even at the same temperature. This suggests that the material expansion is unlikely to be the cause for the recorded higher frictional torque.

Table 4. Temperatures of bearings and lubricants recorded during the tests on the FE8.

Lubricant Tag	Maximum Temperature Bearing [°C]	Torque Value [Nm] at 96 °C Bearing Temperature	Steady State Temperature Bearing [°C]	Maximum Temperature Lubricant [°C]
HR	96–97	12.8–17.5	95	72
LR1	100	20.9	90–100	75
LR2	106–112	21.2–22.2	100	85

3.2. Metallographic Analysis of the Bearings

The condition of the bearings after the tests are summarised in Table 3 and are based on the metallographic analysis results. Bearings from the LR1-1 test, with a duration of approx. 159 h, are shown in Figure 6. Every washer of the two bearings displays pitting, whereas one of the four washers exhibits a spalling, occurring at the surface. Each washer is cut and analysed with respect to WEC (Figure 7). However, WEC features are only found in the spalled washer (housing washer of the test head sided bearing). Three of the four washers from the test run LR2-1 display severe spalling at 72 h. An analysis concerning WEC took place in the test head-sided bearing and WEC was confirmed in the housing washer. Only minor pitting using the LR2 test was observed at 32 h (LR2-2), using the signal of the sound sensor. Nevertheless, WEC was confirmed in the housing and shaft washer of the motor-sided bearing (Figure 8). WEC was confirmed as well in both bearings, respectively, in the housing washers being stopped at 25 h (LR2-3), and, moreover, accompanied by visible ruptures and cracks identified at the surface. In comparison, WEC was not found in a bearing lubricated with LR2 after 20 h of running time (LR2-4).

The FE8 test runs solely lubricated with PAO ended after approx. 160 h (HR1) and 137 h (HR2) by exceeding the torque threshold as a test stop criterion. In both cases, massive surface spalling of the motor sided bearing is observed. No WEC are found within these bearings despite the severe damage of the material.

Further analysis using SEM on the bearings from LR2-5 and HR3 reveals different features on their surfaces (see in Figure 9). In the case of LR2-5, segregated pads are visible on the outer and inner wear track of the bearing. These pads are mostly elongated in shape, with a size of approx. 1–5 × 5–10 μm. The pads seem to be raised from the surrounding metal surface, which has in terms of the area a minor share. In contrast, no similar features are observed on the bearing washers lubricated with PAO (HR3) and on the inner race track of bearing washers from LR2-5 (Figure 9).
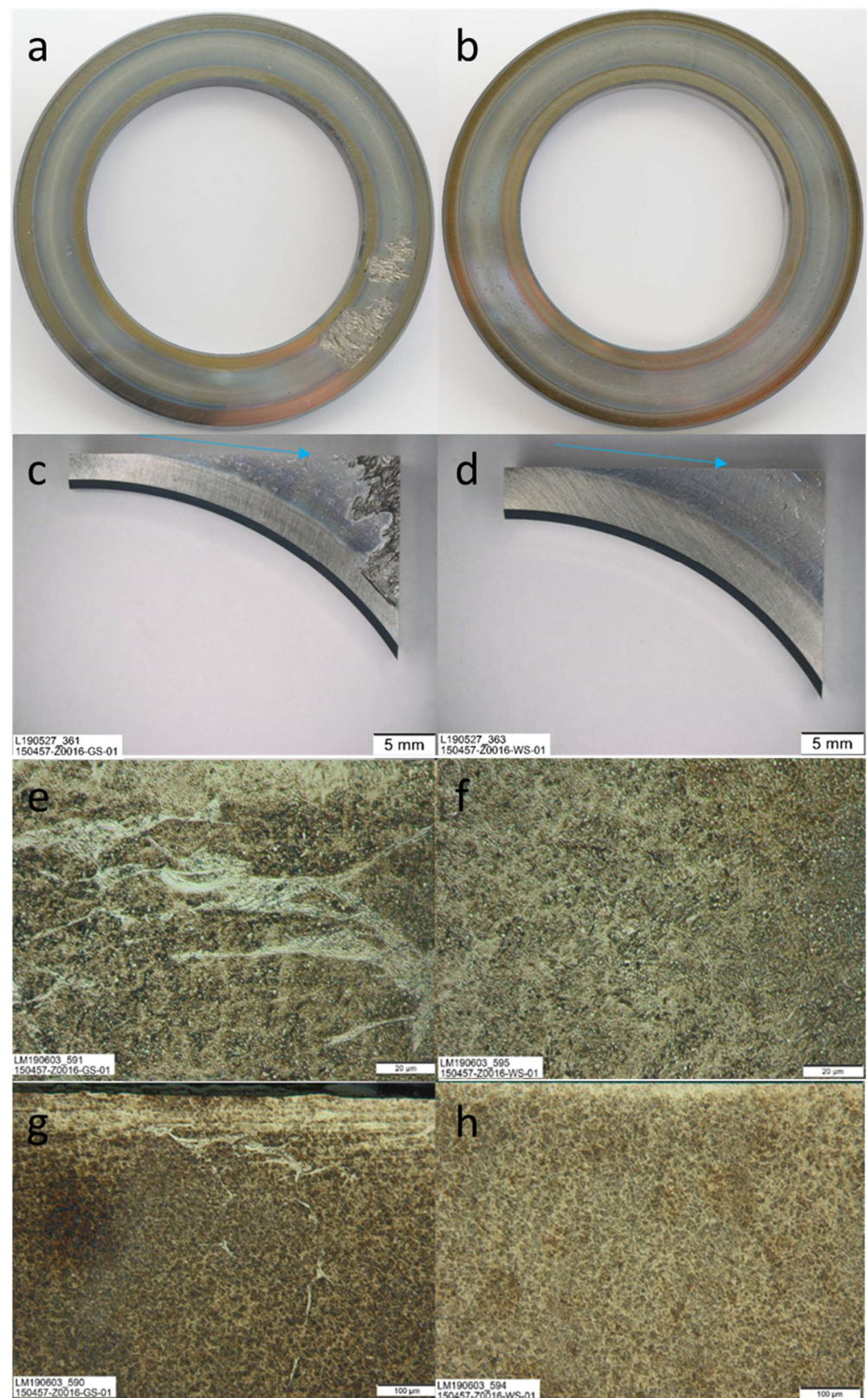
Figure 6. Metallographic analysis of a bearing out of the test run LR1-1 (test head side): Upper row: Overview of the bearings with a massive spalling of the housing washer (**a**) and pittings on the shaft washer (**b**). Cut of housing washer (**c**) and shaft washer (**d**) with blue arrows marking the analysed area on the sawn surface (**second row**). Analysed area of housing washer (**e,g**) and shaft washer (**f,h**) etched 15 s in Nital. WEC was identified in the housing washer.
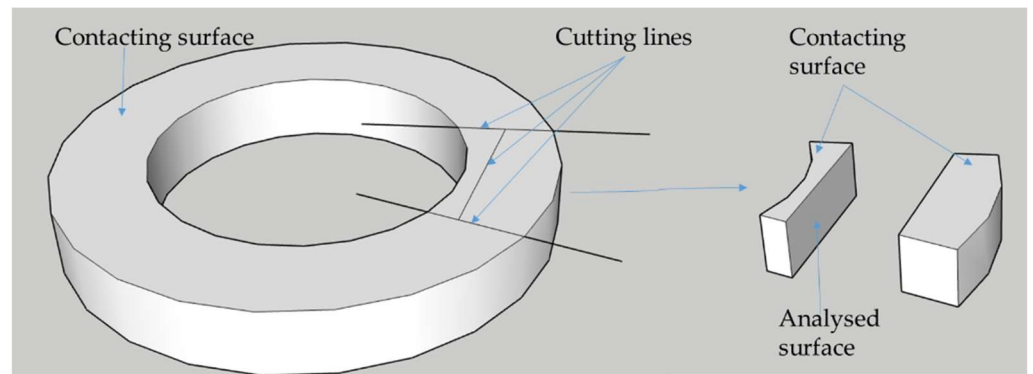
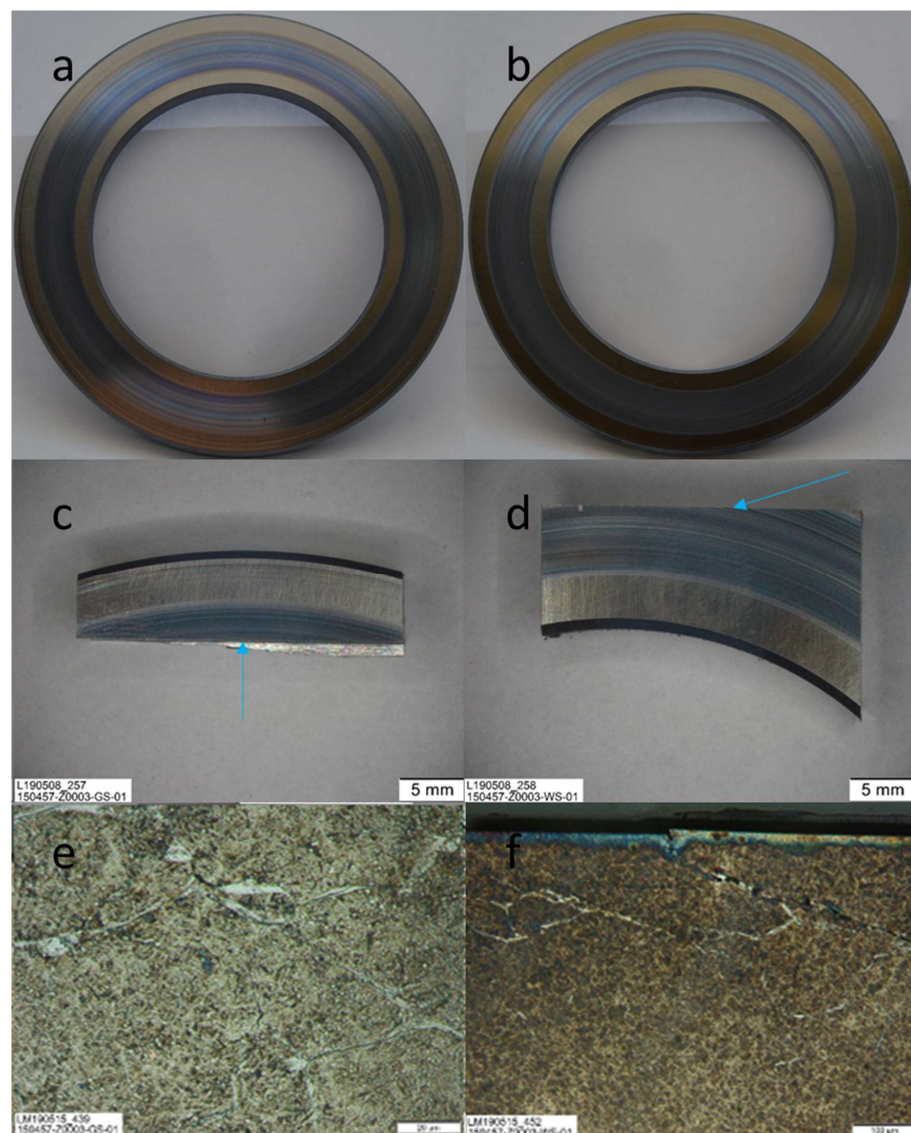**Figure 7.** Schematic representation of the bearing preparation in front of the analysis for WEC features.

Figure 8. Metallographic analysis of a bearing out of the test run LR2-2 (motor side): Upper row: Overview of the housing (**a**) and shaft (**b**) washer with minor pitting on the surface. Cut of housing washer (**c**) and shaft washer (**d**) with blue arrows marking the analysed area on the sawn surface (**second row**). Analysed area of housing washer (**third row, e**) and shaft washer (**third row, f**) etched 15 s in Nital. WEC in both washers identified.
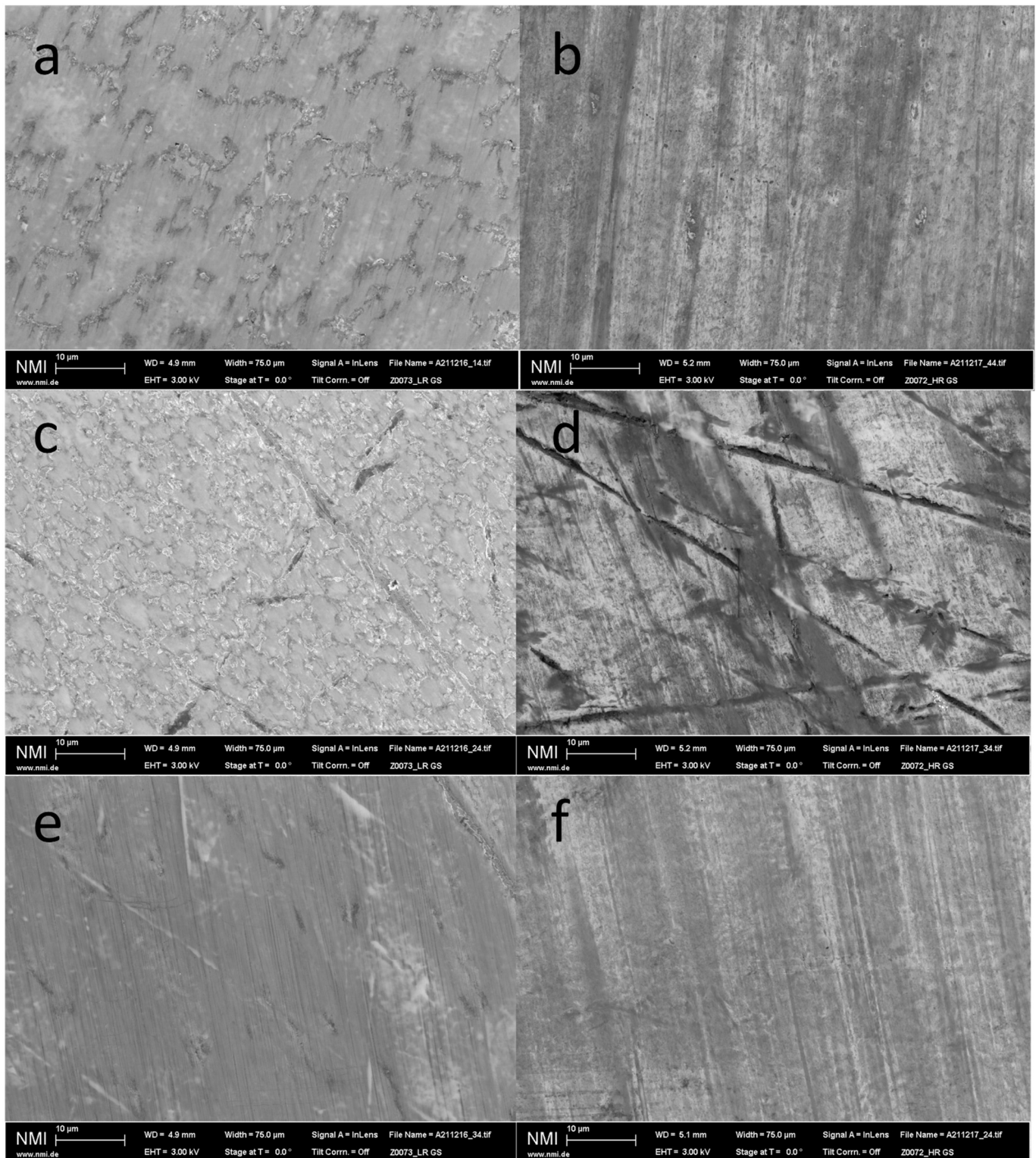
Figure 9. SEM pictures of washers out of the tests LR2-5 (**left, a,c,e**) and HR 3 (**right, b,d,f**). The pictures are taken from the outer racing track (**first row, a,b**), the central running track (**middle row, c, d**) and the inner running track (**third row, e,f**). Tribofilm patches by the use of LR2 lubricant are visible at the outer and central running track of the housing washer.

3.3. EDX and SNMS Analysis

EDX measurements show elevated contents for S and Zn in the case of the LR2-5 bearings in comparison to HR3 bearings and both show an elevated content of oxygen.

Despite no Zn and P components in the original HR3 lubricant, the EDX shows these elements on the bearing washer surface after the test being lubricated by HR3. EDX mapping shows a more inhomogeneous distribution of S, Zn and P in the case of LR2-5 compared to HR3 (Figure 10).
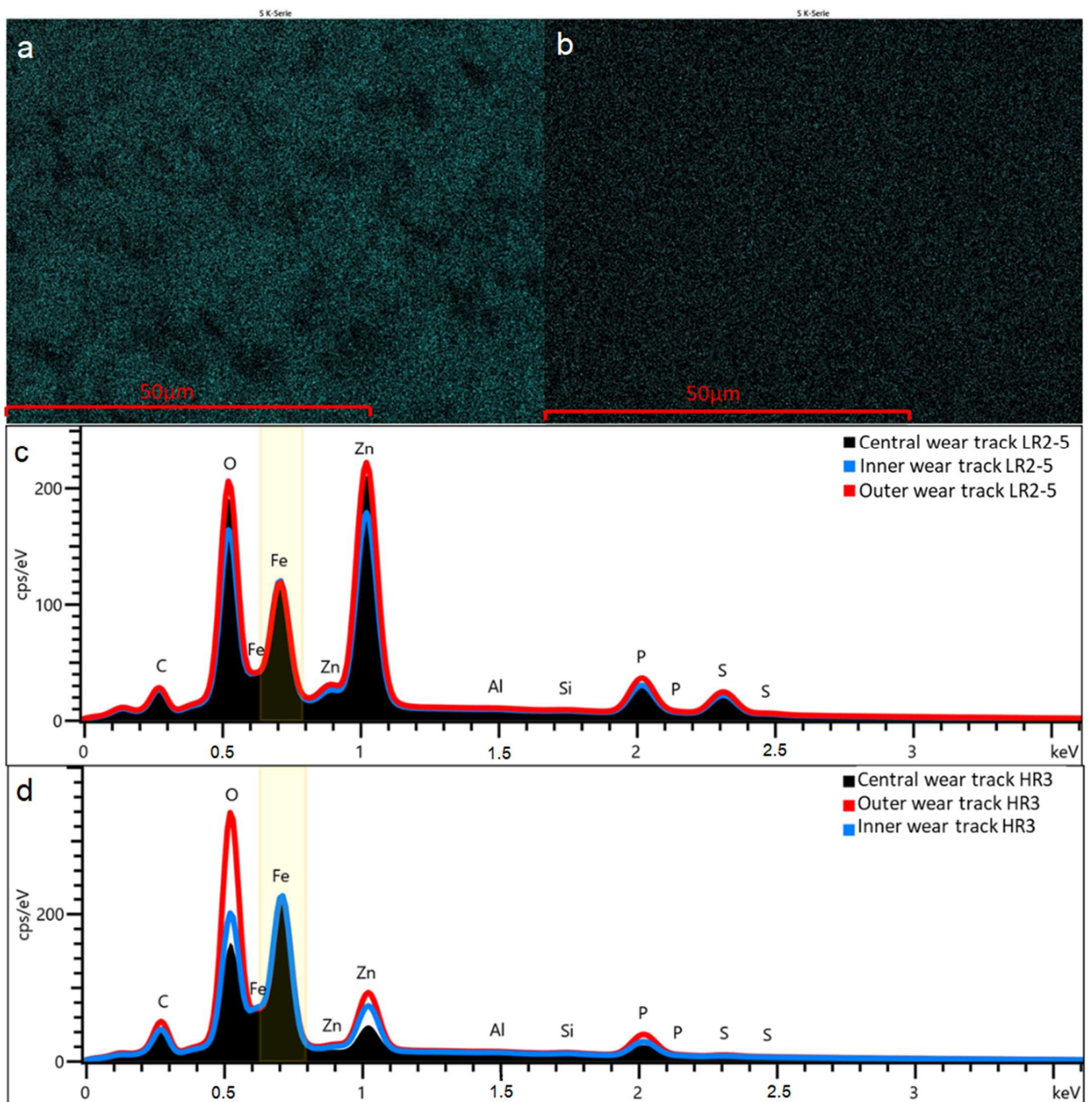

Figure 10. Upper row: EDX mapping picture exemplary for sulphur and the outer running tracks of bearing washer surface of LR2-5 (**a**) and HR 3 (**b**). Comparison of EDX spectra of bearing surfaces LR2-5 (**c**, **middle row**) and HR3 (**d**, **third row**).

The SNMS results are shown in (Figure 11). In order to obtain comparable depth profiles, the raw data was taken with reference to the iron signal. SNMS shows clearly the tribofilm formation in the case of LR2-5. Elevated concentrations of the elements S, P, O and

OH-species are found up to a depth of approx. 50 nm. In addition, C and N are identified to be on these washers however rapidly drop compared to S, P, O and OH. Moreover, atomic hydrogen is found, similar to the concentration profiles of S, P, O and OH. In contrast to EDX analysis, no signal for P was found for the HR3 sample (Figure 11).
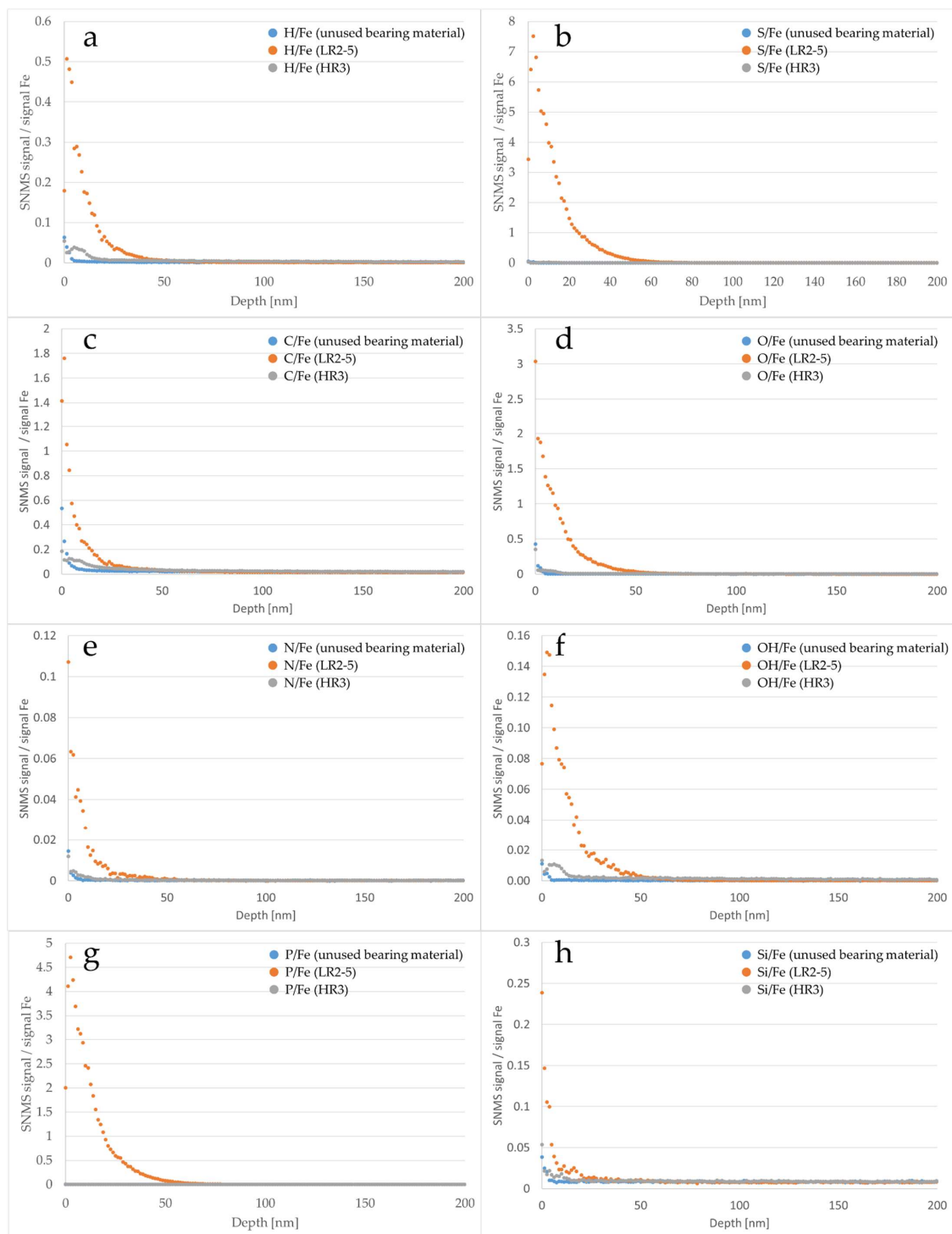
Figure 11. SNMS results for LR2-5 and HR3 compared with a virgin bearing washer sample for the elements/species (**a**): H, (**b**): S, (**c**): C, (**d**): O, (**e**): N, (**f**): OH, (**g**): P and (**h**): Si. Raw Signals of the elements are normalized, dividing the signal by those of Fe. Sputtering took place starting from wear track/washer surface until a depth of 2500 nm. As there were no changes recognized in a deeper depth, only the first 200 nm are displayed.

4. Discussion

The investigations show that the FE8 test rig is suitable to reproduce WEC bearing failure without hydrogen charging or applying an artificial current as already reported earlier [7,10,13,15,17,20]. The use of a low reference lubricant consisting of two components, PAO and ZDDP (LR1), results in the formation of WEC with subsequent bearing damage, supported by the literature as well [11]. Adding DCHA (LR2) has halved the time for this outcome (LR2-1 in Table 3). Further investigations have shown that this low reference lubricant (containing PAO/ZDDP/DCHA) has resulted in WEC formation at a much earlier testing duration, i.e., third of the running time of complete bearing destruction (LR2-3, 25 h running time), whereas in a test stopped five hours earlier (LR2-4) no WEC features were found (Table 3). The investigations on the reasons for torque differences took place far before the occurrence of typical WEC features at 3 h running time. Figure 12 summarises the timeline of low reference test runs.
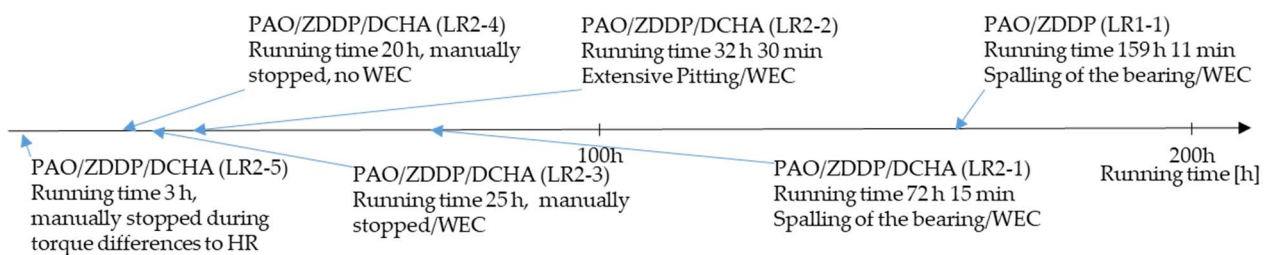

Figure 12. Overview running times of low reference lubricants.

The bearing analysis of the two test runs lubricated with PAO (HR1, HR2), and although severe surface damages were presented, we can confirm there was no WEC formed in the subsurface, which is in agreement with those reported in the literature [15].

The film-forming behaviour of ZDDP as observed by SEM and EDX is well-described in the literature for initiation thermally or tribologically. Thermally induced film formation temperatures beyond 100 °C are reported to be necessary [27], with only little precipitation before a time span of 6 h [28]. In contrast, the tribofilm formation of ZDDP takes place fast and already at lower temperatures [29]. The finding of a patchy tribofilm after 3 h of testing time is well described since ZDDP forms distinctly segregated pads, first with a thickness of approximately 50–150 nm and smoothening as soon as the rubbing time continues [30]. The observation of increased friction indicated by frictional torque in the test runs is well recognised within the timespan of tribofilm formation as friction is described to increase and later drops as soon as a stable tribofilm is formed [31]. The hydrogen identified by SNMS could be the result of rubbing the patchy tribofilms, similar to that as reported in the literature [32] and [33]. It is therefore likely that the patchy tribofilm generated by the ZDDP containing low-reference lubricants enhances friction and thus hydrogen generation. Furthermore, sulphur segregates at grain boundaries stabilising the pinning of hydrogen [14,34]. This poisoning property is similar to the studies carried out by electrolytic charging to study the influence of hydrogen on WEC formation [35–37]. The formation of a patchy tribofilm thus most likely facilitates the hydrogen formation, pinning and acting as a proliferation source for migration into the steel by penetration. Even though no Zn and P were present in the HR3 lubricant, those elements were found in the EDX analysis on the bearing washer lubricated with HR3. Wear of the brass cage is very likely the cause for the presence of Zn. P, however, was not found in the SNMS, and could be a contamination in sample preparation for EDX, as already stated. Further investigation will be conducted to confirm this.

DCHA accelerates the WEC damage significantly (Figure 12), most likely according to the fact that nitrogen-containing additives such as succinimide [29] or ethoxylated tertiary amines [31] are able to remove ZDDP tribofilms. A mechanism involving an interaction between the two dative electrons in the nitrogen acts as a Brønsted base, whereas the

tribofilm acting as a Brønsted acid is suggested [31]. It may also be that DCHA leads to a delay in forming uniformed tribofilm, keeping friction at an elevated level, prolongs hydrogen formation and provides uncovered metal surfaces for hydrogen to penetrate.

Possible sources for the elevated hydrogen content in the case of LR2-5 are water or hydrocarbons in the lubricant. It has been shown from experiments using deuterium oxide in concentrations between 2400 and 6500 ppm that water may act as a source for hydrogen [12]. Considering the very low water contents in front of the tests and also afterwards, it seems much more likely that hydrogen is formed by lubricant decomposition, which is also described in the literature [32,33,38].

It is well known and supported by several theories, that hydrogen can weaken the mechanical properties of steel due to hydrogen embrittlement (HE) [39]. In the current literature, the hydrogen-enhanced decohesion mechanism (HEDE) and the hydrogen-enhanced localized plasticity mechanism (HELP) are often used to describe HE phenomena. The HEDE mechanism suggests that hydrogen causes an atomic separation of the metal by reduction of cohesive metallic interatomic interaction. Paired with tensile stress an atomic separation can occur. The observation of intergranular fracture supports the HEDE, as hydrogen segregates at grain boundaries, reduces interaction between metal atoms and thus leads to intergranular fracture. Reducing the interatomic interdependencies however, has not been demonstrated experimentally until now. In contrast to HEDE, plasticity plays an important role in HELP. In this mechanism, hydrogen is suggested to ease the proliferation and motion of dislocations, leading to local dislocation pile-ups and causing a premature failure of the material. The HELP is supported by experimental evidence as increased dislocation mobility was observed in the presence of hydrogen with in situ transmission electron microscopy experiments [39]. The application of these hydrogen embrittlement models to WEC formation is still under debate [7,10]. The study [40] connects the hydrogen-induced increase of the dislocation mobility caused by rolling contact fatigue with WEA. By reaching a critical dislocation density at obstacles such as carbides, in combination with increased stress concentration due to slip localisation, a dissolution of carbides can be provoked. After that, the clustered dislocations can be redistributed to cell structures with carbon diffusing to the cell boundaries. This WEA formation by dislocation assisted carbon migration with dislocation mobility greatly affected by hydrogen is also modelled by [41]. However, hydrogen is found only to be present in the tribofilm formed. An increased concentration of hydrogen until a depth of 2.5 μm was not found within the 3 h bearing sample. Further work should be done to analyse tribofilm conditions in the timespan of converging friction torque values at approx. 10 h running time. In addition, the hydrogen content of the bulk material by thermal desorption spectrometry should be undertaken to determine the possible influence of hydrogen in the damage mechanism.

The practical implications of this study are a careful evaluation of additives in a way not to cause a patchy tribofilm. Instead, additives have to be preferred leading to a homogeneous reaction layer. Care should also be taken in what way additives or impurities may impair each other to avoid a delay in the formation of the uniform tribofilm formation.

5. Conclusions

Differences in frictional torque values occur in the very early stages of the WEC formation process with significant higher torque values for ZDDP containing low-reference lubricants. It turns out that these differences in frictional torque are accompanied by the formation of a patchy tribofilm. The observation of high torque in all cases by use of a low- reference oil (LR1, LR2) is addressed to the formation of patchy tribofilms within the running period. The lateral interruption of these films is addressed to the competition in film formation by the additives, which means that the film formation in the critical running-in period is interrupted. It is reported that competition between additives, e.g., corrosion protection, anti-wear or extreme pressure additives and could lead to such facts. As the friction locally changes from patch to patch, high and inconsistent friction is the consequence. The high friction itself provides the energy needed to cleave the lubricant

down to fragments and aligned with the formation of hydrogen. In contrast to earlier reports, the hydrogen formation is not seen as a consequence of mixed friction by metal to metal contact, instead by the friction caused by the patchy layers. This assumption is proven by the fact that even though the HR lubricant is exposed to the same conditions as that of the LR1, hydrogen is not found to be higher than the virgin material, thus disproving hydrogen release due to metal–metal rubbing. Even though the hydrogen is missed in the depth > 1000 nm of the material, its significant creation near the surface in the LR case is an unneglectable source for penetration into the depth.

Author Contributions: Conceptualization, J.W.; methodology, J.W., W.H. and L.W.; validation, J.W., W.H., L.W., T.L., P.A. and B.R.; investigation, J.W.; resources, J.W., W.H. and L.W.; data curation, J.W., T.L., P.A. and B.R.; writing—original draft preparation, J.W.; writing—review and editing, W.H., L.W. and P.A.; visualization, J.W.; supervision, L.W. and W.H.; project administration, J.W., L.W. and W.H. All authors have read and agreed to the published version of the manuscript.

Institutional Review Board Statement: Not applicable.

Informed Consent Statement: Not applicable.

Data Availability Statement: Not applicable.

Conflicts of Interest: The authors declare no conflict of interest.

References

1. Scott, D.; Loy, B.; Mills, G.H. Paper 10: Metallurgical Aspects of Rolling Contact Fatigue. *Proc. Inst. Mech. Eng. Conf. Proc.* **1966**, *181*, 94–103. [CrossRef]
2. Gegner, J.; Nierlich, W. Frictional Surface Crack Initiation and Corrosion Fatigue Driven Crack Growth. In *Wind Turbine Tribology Seminar*; NREL: Broomfield, CO, USA, 2011.
3. Tamada, K.; Tanaka, H. Occurrence of brittle flaking on bearings used for automotive electrical instruments and auxiliary devices. *Wear* **1996**, *199*, 245–252. [CrossRef]
4. Kino, N.; Keizo, O. The influence of hydrogen on rolling contact fatigue life and its improvement. *JSAE Rev.* **2003**, *24*, 289–294. [CrossRef]
5. Harada, H.; Mikami, T.; Shibata, M.; Sokai, D.; Yamamoto, A.; Tsubakino, H. Microstructural changes and crack initiation with white etching area formation under rolling/sliding contact in bearing steel. *ISIJ Int.* **2005**, *45*, 1897–1902. [CrossRef]
6. Gegner, J. *Tribological Aspects of Rolling Bearing Failures*; InTech: Rijeka, Croatia, 2011; pp. 33–94.
7. Evans, M.H.; Richardson, A.D.; Wang, L.; Wood, R.J.K. Serial sectioning investigation of butterfly and white etching crack (WEC) formation in wind turbine gearbox bearings. *Wear* **2013**, *302*, 1573–1582. [CrossRef]
8. Pérez, J.M.P.; Márquez, F.P.G.; Tobias, A.; Papaelis, M. Wind turbine reliability analysis. *Renew. Sustain. Energy Rev.* **2013**, *23*, 463–472. [CrossRef]
9. Evans, M.H. An updated review: White etching cracks (WECs) and axial cracks in wind turbine gearbox bearings. *Mater. Sci. Technol.* **2016**, *32*, 1133–1169. [CrossRef]
10. López-Uruñuela, F.J.; Fernández-Díaz, B.; Pagano, F.; López-Ortega, A.; Pinedo, B.; Bayón, R.; Aguirrebeitia, J. Broad review of "White Etching Crack" failure in wind turbine gearbox bearings: Main factors and experimental investigations. *Int. J. Fatigue* **2021**, *145*, 106091. [CrossRef]
11. Gould, B.; Demas, N.G.; Pollard, G.; Rydel, J.J.; Ingram, M.; Greco, A.C. The effect of lubricant composition on white etching crack failures. *Tribol. Lett.* **2018**, *67*, 7. [CrossRef]
12. Haque, T.; Korres, S.; Carey, J.T.; Jacobs, P.W.; Loos, J.; Franke, J. Lubricant effects on white etching cracking failures in thrust bearing rig tests. *Tribol. Trans.* **2018**, *61*, 979–990. [CrossRef]
13. Pape, F.; Terwey, J.T.; Wiesker, S.; Averbeck, S.; Muhmann, C.; Lipinsky, D.; Arlinghaus, H.F.; Kerscher, E.; Sauer, B.; Poll, G. Tribological research on the development of White Etching Cracks (WECs). *Forsch. Im Ing.* **2018**, *82*, 341–352. [CrossRef]
14. Richardson, A.; Evans, M.-H.; Wang, L.; Ingram, M.; Rowland, Z.; Llanos, G.; Wood, R. The effect of over-based calcium sulfonate detergent additives on white etching crack (WEC) formation in rolling contact fatigue tested 100Cr6 steel. *Tribol. Int.* **2019**, *133*, 246–262. [CrossRef]
15. Holweger, W.; Wolf, M.; Merk, D.; Blass, T.; Goss, M.; Loos, J.; Barteldes, S.; Jakovics, A. White etching crack root cause investigations. *Tribol. Trans.* **2015**, *58*, 59–69. [CrossRef]

16. Ruellan, A.; Stadler, K.; Rydel, J.J.; Ryan, H. The influence of lubricant formulation on early thrust and radial bearing damage associated with white etching cracks. *Proc. Inst. Mech. Eng. Part J J. Eng. Tribol.* **2020**, *235*, 1047–1059. [CrossRef]

17. Diederichs, M.; Barteldes, S.; Schwedt, A.; Mayer, J.; Holweger, W. Study of subsurface initiation mechanism for white etching crack formation. *Mater. Sci. Technol.* **2016**, *32*, 1170–1178. [CrossRef]

18. Franke, J.; Carey, J.T.; Korres, S.; Haque, T.; Jacobs, P.W.; Loos, J.; Kruhoeffer, W. White etching cracking—Simulation in bearing rig and bench tests. *Tribol. Trans.* **2018**, *61*, 403–413. [CrossRef]

19. Guzmán, F.G.; Oezel, M.; Jacobs, G.; Burghardt, G.; Broeckmann, C.; Janitzky, T. Reproduction of white etching cracks under rolling contact loading on thrust bearing and two-disc test rigs. *Wear* **2017**, *390*, 23–32. [CrossRef]

20. Linzmayer, M.; Sous, C.; Guzmán, F.G.; Jacobs, G. Round robin test for the damage reproduction of white etching crack in cylindrical roller thrust bearings. *Wear* **2021**, *480*, 203925. [CrossRef]

21. Spille, J.; Wranik, J.; Barteldes, S.; Mayer, J.; Schwedt, A.; Zürcher, M.; Lutz, T.; Wang, L.; Holweger, W. A study on the initiation processes of white etching cracks (WECs) in AISI 52100 bearing steel. *Wear* **2021**, *477*, 203864. [CrossRef]

22. *DIN 51819-3*; Prüfung von Schmierstoffen—Mechanisch-dynamische Prüfung auf dem Wälzlagerschmierstoff-Prüfgerät FE8—Teil 3: Verfahren für Schmieröl—einzusetzende Prüflager: Axialzylinderrollenlager. Deutsches Institut für Normung e.V.: Beuth, Germany, 2016.

23. Schaeffler Technologies AG & Co. *DIN 51819*; KG, Manual Test rig FE8; Schaeffler Technologies AG & Co.: Schweinfurt, Germany, 2017.

24. Gold, P.W.; Loos, J.; Kuhn, M. Leistungsfähige PVD-Wälzlagerbeschichtungen. In *Materialwissenschaft und Werkstofftechnik: Entwicklung, Fertigung, Prüfung, Eigenschaften und Anwendungen technischer Werkstoffe*; Wiley-VCH GmbH: Weinheim, Germany, 2003; Volume 34, pp. 919–923.

25. Hamrock, J.; Dowson, D. *Applications of Film Thickness Equations*; NASA Technical Memorandum 81701; NASA: Cleveland, OH, USA, 1983.

26. Rudnick, L.R. *Lubricant Additives Chemistry and Applications*; CRC Press: Boca Raton, FL, USA, 2009.

27. Bancroft, G.M.; Kasrai, M.; Fuller, M.; Yin, Z.; Fyfe, K.; Tan, K.H. Mechanisms of tribochemical film formation: Stabilityof tribo-and thermally-generated ZDDP films. *Tribol. Lett.* **1997**, *3*, 47–51. [CrossRef]

28. Fuller, M.L.S.; Kasrai, M.; Bancroft, G.M.; Fyfe, K.; Tan, K.H. Solution decomposition of zinc dialkyl dithiophosphate and its effect on antiwear and thermal film formation studied by X-ray absorption spectroscopy. *Tribol. Int.* **1998**, *31*, 627–644. [CrossRef]

29. Fujita, H.; Glovnea, R.; Spikes, H. Study of zinc dialkydithiophosphate antiwear film formation and removal processes, part I: Experimental. *Tribol. Trans.* **2005**, *48*, 558–566. [CrossRef]

30. Aktary, M.; McDermott, M.; McAlpine, G. Morphology and nanomechanical properties of ZDDP antiwear films as a function of tribological contact time. *Tribol. Lett.* **2002**, *12*, 155–162. [CrossRef]

31. Dawczyk, J.U. *The Effect of Organic Friction Modifiers on zddp Tribofilm*; Imperial College: London, UK, 2018.

32. Kohara, M.; Kawamura, T.; Egami, M. Study on mechanism of hydrogen generation from lubricants. *Tribol. Trans.* **2006**, *49*, 53–60. [CrossRef]

33. Lu, R.; Minami, I.; Nanao, H.; Mori, S. Investigation of decomposition of hydrocarbon oil on the nascent surface of steel. *Tribol. Lett.* **2007**, *27*, 25–30. [CrossRef]

34. Esfahani, E.A.; Soltanahmadi, S.; Morina, A.; Han, B.; Nedelcu, I.; van Eijk, M.C.; Neville, A. The multiple roles of a chemical tribofilm in hydrogen uptake from lubricated rubbing contacts. *Tribol. Int.* **2019**, *146*, 106023. [CrossRef]

35. Szost, A.; Rivera-Diaz-del-Castillo, P.E.J. Unveiling the nature of hydrogen embrittlement in bearing steels employing a new technique. *Scr. Mater.* **2013**, *68*, 467–470. [CrossRef]

36. Vegter, R.H.; Slycke, J.T.; Beswick, J.; Dean, S.W. *The Role of Hydrogen on Rolling Contact Fatigue Response of Rolling Element Bearings*; ASTM International: West Conshohocken, PA, USA, 2010; Volume 7.

37. Ruellan, A. Tribological Analysis of White Etching Crack (WEC) Failures in Rolling Element Bearings. Mechanics of Materials [physics.class-ph]. Ph.D. Thesis, INSA de Lyon, Lyon, France, 2014.

38. Stadler, K.; Lai, J.; Vegter, R. A Review: The Dilemma with Premature White Etching Crack (WEC) Bearing Failures. In *Bearing Steel Technologies: 10th Volume, Advances in Steel Technologies for Rolling Bearings*; ASTM International: West Conshohocken, PA, USA, 2014; pp. 487–508.

39. Xinfeng, L.; Xianfeng, M.; Zhang, J.; Akiyama, E.; Wang, Y.; Song, X. Review of Hydrogen Embrittlement in Metals: Hydrogen Difusion, Hydrogen Characterization, Hydrogen Embrittlement Mechanism and Prevention. *Acta Metall. Sin.* **2019**, *33*, 759–773.

40. Oezel, M.; Schwedt, A.; Janitzky, T.; Kelley, R.; Bouchet-Marquis, C.; Pullan, L.; Mayer, J. Formation of white etching areas in SAE 52100 bearing steel under rolling contact fatigue–Influence of diffusible hydrogen. *Wear* **2018**, *414*, 352–365. [CrossRef]

41. Liang, X.Z.; Rivera-Díaz-del-Castillo, P.E. Hydrogen-accelerated white etching area formation in bearings under rolling contact fatigue. *Int. J. Fatigue* **2022**, *159*, 106753. [CrossRef]